TEST REPORT

RANGER DYNAMIC PERFORMANCE MEASUREMENTS

Prepared by: Space Systems Laboratory
University of Maryland
College Park, MD 20742

SSL Document Number: DT21-0041

Submission Date: January 2006

Inquiries to: Stephen Roderick or Walter Smith
Telephone: 301-405-6954 or 3301-405-1906
Fax: 301-405-2918
e-mail: roderick@ssl.umd.edu or
wsmith@ssl.umd.edu

Space Systems Laboratory
University of Maryland

1.0 Introduction

This report documents the results for testing the Ranger robotic dexterous manipulator system for per Test Procedure DT21-0040. All testing took place at the University of Maryland's Space Systems Laboratory (UMD/SSL).

2.0 Equipment

The test article was the Ranger left dexterous manipulator assembly (DXL for DeXterous Left), SSL part number FD07-0400. Data for positioning was collected with a Faro portable CMM Platinum Series (Model Number P0802, Serial Number P08020503418).

For the bandwidth measurements, the right dexterous arm (DXR) was used. Data was collected with a Keyence Laser Displacement Sensor (Model Number LB-70, Serial Number 051257).

2.1 Hardware setup

2.1.1 Positioning Faro arm

Mounting the measurement system took consideration of various requirements. The end result was a compromise of the most important needs.

2.1.1.1 Provide adequate mount for Faro arm base

Ultimately, the Faro base was mounted on the top of the head as shown in Figure 1, which provides a stiff area that does not allow relative motion between the Faro arm and the Ranger arm. The head provides a convenient clamping flange with room enough for two clamps.

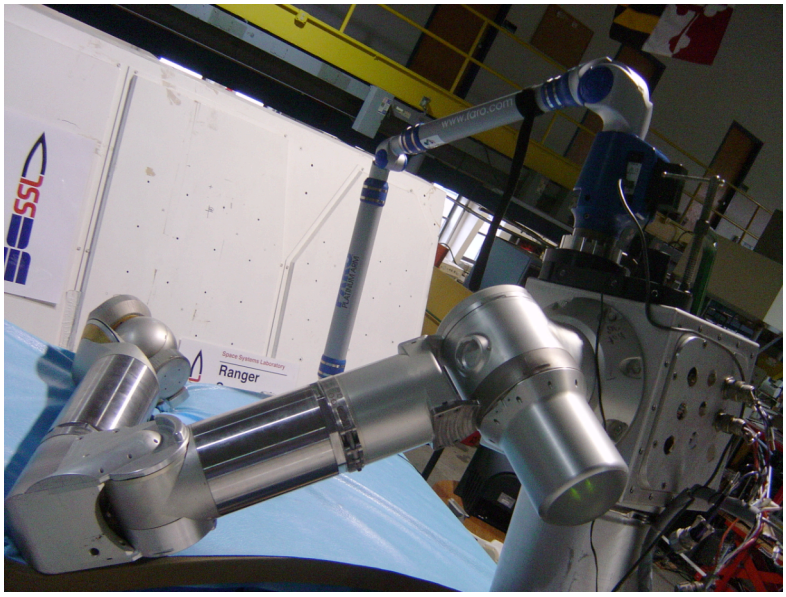

Figure 1: Test set-up

2.1.1.2 Match work volumes as much as possible

By mounting the Faro base on the head the work volumes are roughly matched. The vertical location (Y direction in the head frame)of the Faro arm is slightly higher and the location of the first pitch joint is rotated 90 degrees (about X axis) and offset to the left (+ Z direction). These differences seem to be acceptable as it would be impossible to collocate the arms.

2.1.1.3 Protecting the Faro arm in case of system crash

The Faro arm could not reach the lowest point of the Ranger arm so a table was positioned to catch the arm(s) before the Faro arm could reach a travel limit. Padding is provided to prevent damage to either arm. The Faro arm is oriented to be above (+ Y direction head frame) to prevent damage due to the mass of the Ranger arm.

2.1.1.4 Making sure Faro arm can operate freely in the areas of interest

The Ranger arm was moved to the points of interest at the travel extremes. The Faro arm was then positioned to determine if it could measure that position and not be in danger of approaching either a singularity or a travel limit.

2.1.1.5 Adapting Faro arm probe to Ranger arm

The specification requires a load (2 kg or 4.4 lbs in our case) be mounted outboard of the end of the robot. The weight of the Interchangeable End Effector Mechanism (IEEM) and the tool adapter is approximately 3.7 pounds. The document specifies the center-of-gravity (COG) of this load to be located 4 cm (1.57 in.) along the tool axis and 2 cm (0.78 in.) offset from that axis. If we consider the output flange to be the end of the robot this point is located inside the IEEM. It is assumed this load case tests the effects of eccentric payloads on robot performance. However, Ranger tooling is axis symmetric about the tool axis making the need for eccentric loading not applicable. It is approximated the COG location of the IEEM and tooling adapter is axis symmetric about the tool axis and offset from the output flange approximately 1.75 inches. This offset should provide some measure of the wrist pitch axis stability. This configuration can be refined to better meet the specification if deemed necessary.

A tooling adapter was mounted onto the output flange in order to attach the measurement system. Preliminary testing has shown that an additional degree-of-freedom (DOF) is necessary between the Faro arm and the tooling adapter. However, measurements can be taken if the sampling technique is slow enough to allow human assistance to hold the Faro arm in place.

2.1.1.6 Cancel deflections due to supporting structure

As the Faro arm base moves with the Ranger arm base any errors due to deflecting support structure will be negated.

2.2 Coordinate frame alignment

In order to simplify data reduction, a common coordinate frame was established between DXL and the Faro arm. The base frame of DXL was selected (as shown in Figure 2) as shifting frames on the Faro arm is not difficult. The Faro arm software provides a routine for establishing multiple coordinate frames. The frame of the arm was established in the Faro arm by digitizing the face of the mounting head and the center of the first DOF. This frame was used for all testing except for repeatability.

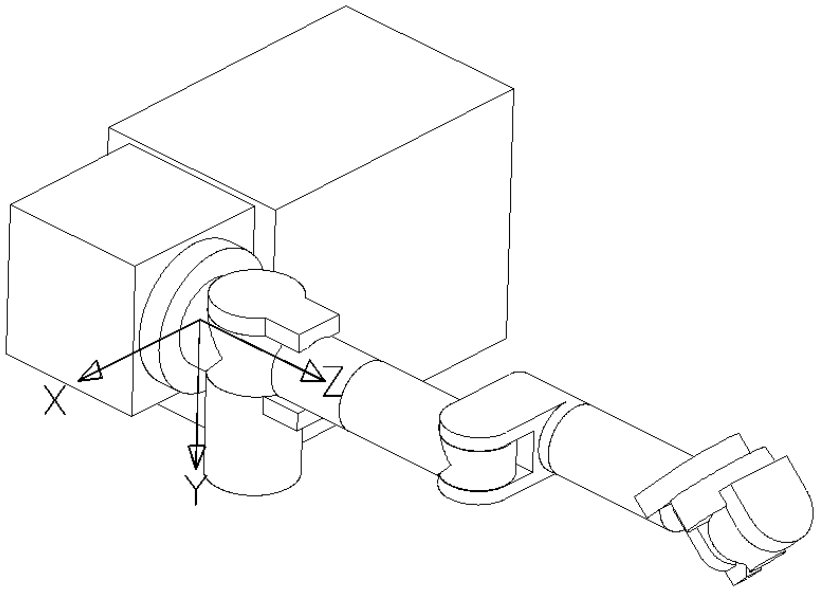

Figure 2: Coordinate frame

For the dynamic tests a frame was established by selecting points on the plane where the data was collected. Using this plane reduces the amount of data manipulation necessary. This frame is referred to as the Mechanical Interface Coordinate System per section 6.3 in ANSI R15.05-2-1992 and described in section 10.2.3.3.

2.3 Measurement tool offset compensation

The Faro arm is intended for measuring geometric features on mechanical hardware. In order to use the Faro arm for measuring the performance of DXL an adapter was fabricated to hold the Faro probe tip to DXL. The normal operation of the Faro has the operator digitize probe locations using a compensation offset for the probe sphere diameter. This requires the operator to digitize a reference feature on DXL for every data point to be collected. This technique proves to be time intensive.

In order to collect the data in a reasonable amount of time, the probe is mounted directly to DXL via the adapter as shown in Figure 3. The final probe connection is related to the location of the arm wrist frame numerically. This relation is established by measuring the relative position between the wrist pitch axis center and the probe center mounted in the adapter. The center of the wrist pitch axis is determined by using the Faro arm and the location of the measuring probe in the adapter is determined by using a non-compensated mode on the Faro arm (Figure 4). Once these two locations are determined an accurate offset for the measuring probe location can be numerically determined. This method reduces the chances for stacked tolerances affecting the measurement precision.

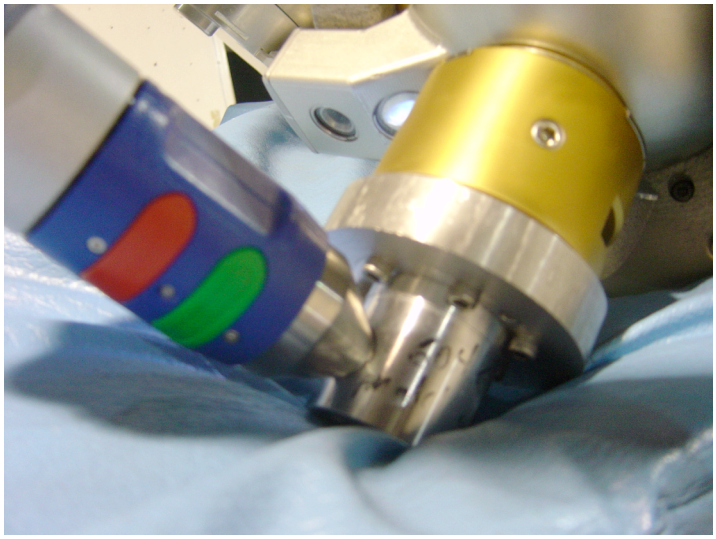

Figure 3: Adapter to hold Faro probe tip to the DXL

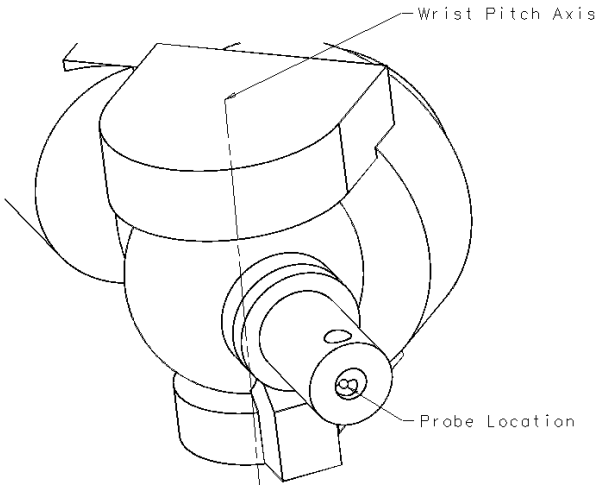

Figure 4: Wrist pitch axis

3.0 Test Results

Table 1: Robot Dynamic Performance Data Report
Reference: ANSI/RIA R15.05-1-1990

Description of data	Units	Section	Class 1 Path prioritize
Constants			
Payload	kg		1.7
Test load category			2
Path dimensions		8.6	
Segment size	mm	8.6	
Programmed speed			100%
Path accuracy		10.2	
Relative			
- maximum, AC_{REL}	mm		4.61
- average. $\mathbf{AC}_{REL}$	mm		0.832
Absolute (optional)			
- maximum, AC_{REL}	mm		
- average. $\mathbf{AC}_{REL}$	mm		
Path reliability		10.3	
Maximum, PR	mm		.86
Average, PR	mm		.26
Cornering deviations		10.4	
Round-off, CR	mm		13.65
Overshoot, CO	mm		14.31
Path/speed relationships		10.5	
Accuracy, AS	mm		
Repeatability, RS	mm		
Fluctuation, FS	mm		
Acceleration time, TS	s		

The path/speed relationship data was not collected as the Faro portable CMM does not time stamp the data.

Bandwidth results are given in the 9 appended files. The raw data is available as data-x_y.log, where x_y is the frequency of the test (e.g. data-0_7.log is for 0.7 Hz). The data has also been imported into Excel and preliminary data reduction has been undertaken. The Excel files are named data-x_y.xls, with x_y being the frequency of the test as above.

The preliminary data reduction, undertaken in all result spreadsheets, only inverts the sense of the measured voltage and calculates the actual sample time periods of the control station software. These values were plotted to graph.

Calibration data is given in calibration.xls. The zero offset was taken as the laser sensor output voltage at the center of the sine wave. The dx/dv slope was taken as the average of the total change in laser sensor output voltage, over the total change in the measured distance of the arm from the laser sensor. Both quantities were averaged over the beginning and end test suite measurements.

The Excel spreadsheets for the 0.7 Hz and the 1.0 Hz data have had further data reduction applied. These spreadsheets also calculate the actual distance in inches, from the laser sensor, based on the measured laser sensor output voltage and the calibration measurements. This was graphed alongside the commanded and actual joint positions, an example of which is given in Figure 5.

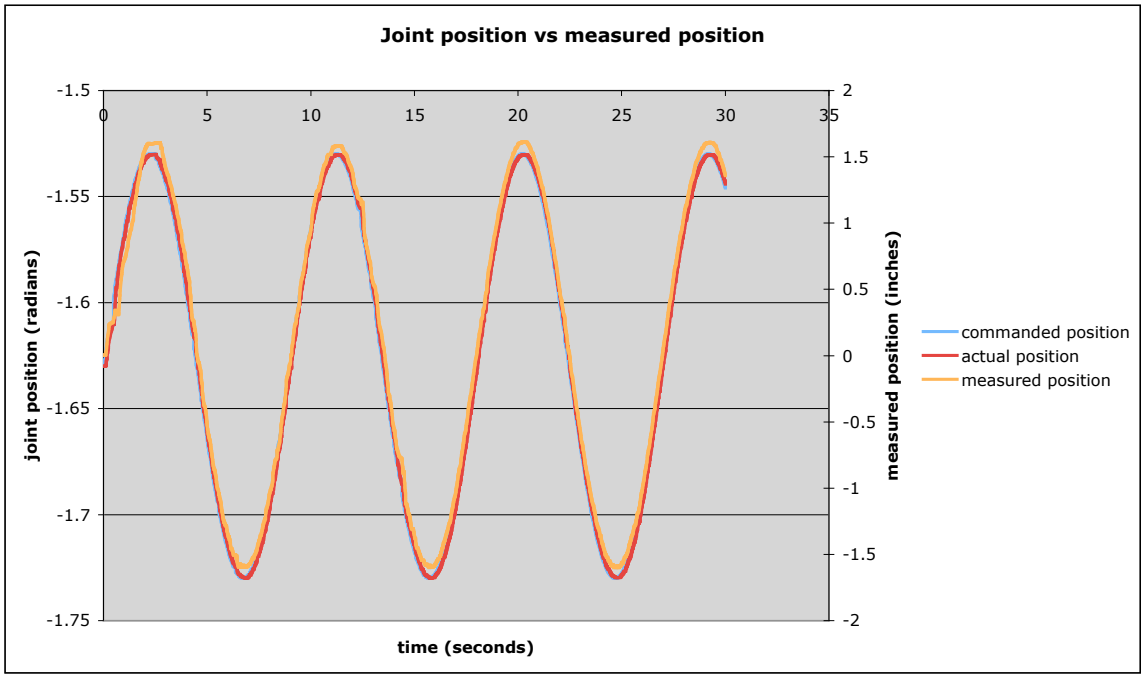

Figure 5: Fully reduced position data, for 0.7 Hz sine wave

The calculated distance is seen to closely follow the commanded and actual positions. Note that there is an offset in time between a commanded position being sent from the control station, and

the associated changed in actual position as reported at the control station. This appears to be on the order of about 20 milliseconds, which agrees with the known network delay, the onboard robot controller running with an 8-millisecond period, and the control station running with a 10-millisecond period.

The graphs of the control station period vividly show the effects of the desktop operating system in use as shown in Figure 6. An average period of 20 milliseconds occurs, which is double the intended 10 milliseconds. Large spikes in the period are also evident. We believe this large variability in the period of the incoming commanded positions to the robot controller are directly responsible for the steps and spikes evident in the commanded and actual joint positions.

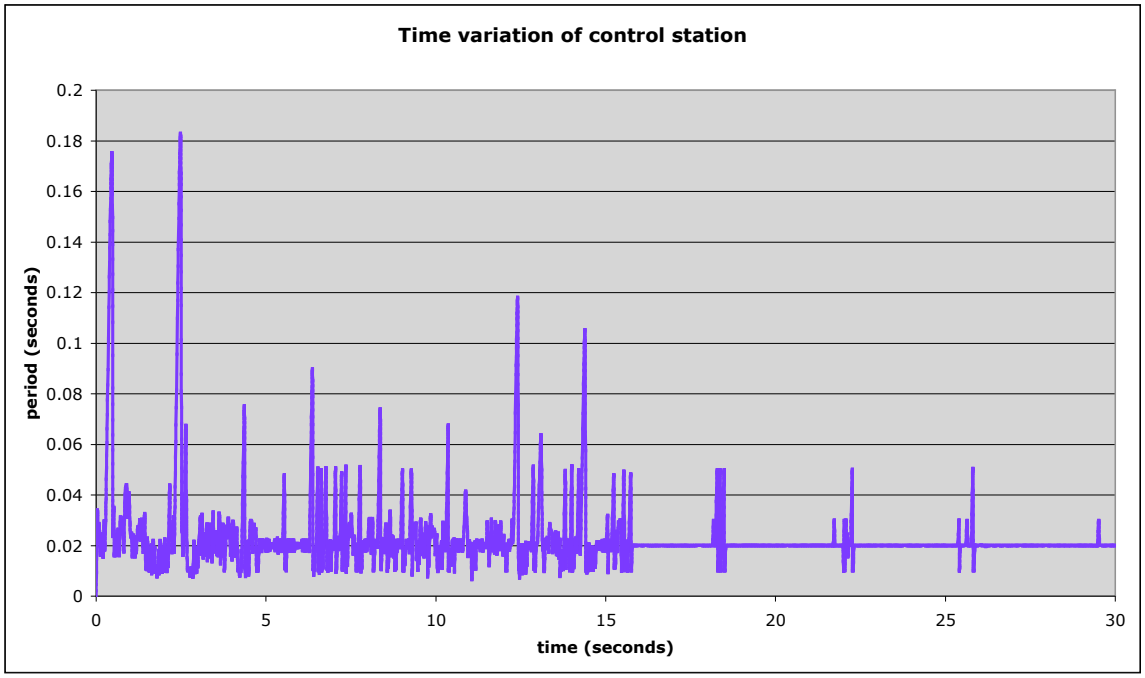

Figure 6: Variation of control station period, for 0.7 Hz sine wave